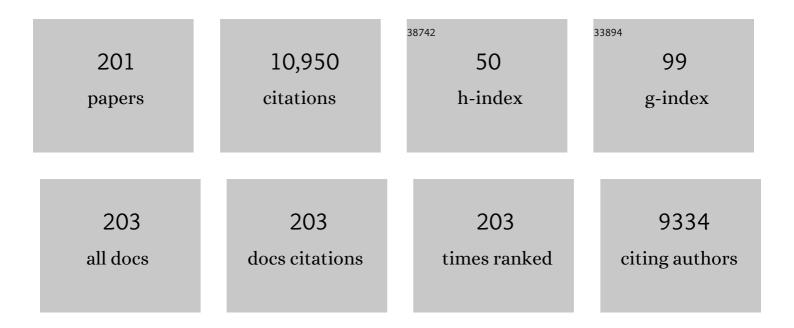
List of Publications by Year in descending order

Source: https://exaly.com/author-pdf/2281336/publications.pdf Version: 2024-02-01



LONG CHULYE

#	Article	IF	CITATIONS
1	NIRS-SPM: Statistical parametric mapping for near-infrared spectroscopy. NeuroImage, 2009, 44, 428-447.	4.2	910
2	Deep Learning COVID-19 Features on CXR Using Limited Training Data Sets. IEEE Transactions on Medical Imaging, 2020, 39, 2688-2700.	8.9	653
3	A deep convolutional neural network using directional wavelets for lowâ€dose Xâ€ray CT reconstruction. Medical Physics, 2017, 44, e360-e375.	3.0	561
4	kâ€ŧ FOCUSS: A general compressed sensing framework for high resolution dynamic MRI. Magnetic Resonance in Medicine, 2009, 61, 103-116.	3.0	536
5	Framing U-Net via Deep Convolutional Framelets: Application to Sparse-View CT. IEEE Transactions on Medical Imaging, 2018, 37, 1418-1429.	8.9	388
6	Statistical analysis of fNIRS data: A comprehensive review. NeuroImage, 2014, 85, 72-91.	4.2	318
7	Compressive MUSIC: Revisiting the Link Between Compressive Sensing and Array Signal Processing. IEEE Transactions on Information Theory, 2012, 58, 278-301.	2.4	292
8	Deep Convolutional Framelets: A General Deep Learning Framework for Inverse Problems. SIAM Journal on Imaging Sciences, 2018, 11, 991-1048.	2.2	243
9	Wavelet minimum description length detrending for near-infrared spectroscopy. Journal of Biomedical Optics, 2009, 14, 034004.	2.6	241
10	Improvedk–tBLAST andk–tSENSE using FOCUSS. Physics in Medicine and Biology, 2007, 52, 3201-3226.	3.0	235
11	Deep learning for tomographic image reconstruction. Nature Machine Intelligence, 2020, 2, 737-748.	16.0	233
12	Comparative study of iterative reconstruction algorithms for missing cone problems in optical diffraction tomography. Optics Express, 2015, 23, 16933.	3.4	226
13	Deep Convolutional Framelet Denosing for Low-Dose CT via Wavelet Residual Network. IEEE Transactions on Medical Imaging, 2018, 37, 1358-1369.	8.9	216
14	Deep Residual Learning for Accelerated MRI Using Magnitude and Phase Networks. IEEE Transactions on Biomedical Engineering, 2018, 65, 1985-1995.	4.2	212
15	Deep learning with domain adaptation for accelerated projectionâ€reconstruction MR. Magnetic Resonance in Medicine, 2018, 80, 1189-1205.	3.0	204
16	{{k} -Space Deep Learning for Accelerated MRI. IEEE Transactions on Medical Imaging, 2020, 39, 377-386.	8.9	193
17	Image Reconstruction: From Sparsity to Data-Adaptive Methods and Machine Learning. Proceedings of the IEEE, 2020, 108, 86-109.	21.3	187
18	A General Framework for Compressed Sensing and Parallel MRI Using Annihilating Filter Based Low-Rank Hankel Matrix. IEEE Transactions on Computational Imaging, 2016, 2, 480-495.	4.4	175

#	Article	IF	CITATIONS
19	Real-time visualization of 3-D dynamic microscopic objects using optical diffraction tomography. Optics Express, 2013, 21, 32269.	3.4	161
20	Cycle onsistent adversarial denoising network for multiphase coronary CT angiography. Medical Physics, 2019, 46, 550-562.	3.0	157
21	A Data-Driven Sparse GLM for fMRI Analysis Using Sparse Dictionary Learning With MDL Criterion. IEEE Transactions on Medical Imaging, 2011, 30, 1076-1089.	8.9	149
22	Enhancement of Terahertz Pulse Emission by Optical Nanoantenna. ACS Nano, 2012, 6, 2026-2031.	14.6	139
23	Annihilating Filter-Based Low-Rank Hankel Matrix Approach for Image Inpainting. IEEE Transactions on Image Processing, 2015, 24, 3498-3511.	9.8	136
24	FALCON: fast and unbiased reconstruction of high-density super-resolution microscopy data. Scientific Reports, 2014, 4, 4577.	3.3	125
25	Sparse-View Spectral CT Reconstruction Using Spectral Patch-Based Low-Rank Penalty. IEEE Transactions on Medical Imaging, 2015, 34, 748-760.	8.9	124
26	Deep residual learning for compressed sensing MRI. , 2017, , .		122
27	Compressed sensing MRI: a review from signal processing perspective. BMC Biomedical Engineering, 2019, 1, 8.	2.6	106
28	Projection reconstruction MR imaging using FOCUSS. Magnetic Resonance in Medicine, 2007, 57, 764-775.	3.0	102
29	CycleMorph: Cycle consistent unsupervised deformable image registration. Medical Image Analysis, 2021, 71, 102036.	11.6	102
30	Quantitative analysis of hemodynamic and metabolic changes in subcortical vascular dementia using simultaneous near-infrared spectroscopy and fMRI measurements. NeuroImage, 2011, 55, 176-184.	4.2	96
31	Efficient B-Mode Ultrasound Image Reconstruction From Sub-Sampled RF Data Using Deep Learning. IEEE Transactions on Medical Imaging, 2019, 38, 325-336.	8.9	94
32	Self-reference quantitative phase microscopy for microfluidic devices. Optics Letters, 2010, 35, 514.	3.3	92
33	Radial kâ€ŧ FOCUSS for highâ€resolution cardiac cine MRI. Magnetic Resonance in Medicine, 2010, 63, 68-78.	3.0	88
34	CollaGAN: Collaborative GAN for Missing Image Data Imputation. , 2019, , .		88
35	Acceleration of MR parameter mapping using annihilating filterâ€based low rank hankel matrix (ALOHA). Magnetic Resonance in Medicine, 2016, 76, 1848-1864.	3.0	83
36	Mumford–Shah Loss Functional for Image Segmentation With Deep Learning. IEEE Transactions on Image Processing, 2020, 29, 1856-1866.	9.8	80

#	Article	IF	CITATIONS
37	Adaptive and Compressive Beamforming Using Deep Learning for Medical Ultrasound. IEEE Transactions on Ultrasonics, Ferroelectrics, and Frequency Control, 2020, 67, 1558-1572.	3.0	79
38	Deep Learning Diffuse Optical Tomography. IEEE Transactions on Medical Imaging, 2020, 39, 877-887.	8.9	77
39	Compressive Diffuse Optical Tomography: Noniterative Exact Reconstruction Using Joint Sparsity. IEEE Transactions on Medical Imaging, 2011, 30, 1129-1142.	8.9	75
40	Motion estimated and compensated compressed sensing dynamic magnetic resonance imaging: What we can learn from video compression techniques. International Journal of Imaging Systems and Technology, 2010, 20, 81-98.	4.1	74
41	Fluorescent microscopy beyond diffraction limits using speckle illumination and joint support recovery. Scientific Reports, 2013, 3, 2075.	3.3	74
42	Nonlinear multigrid algorithms for Bayesian optical diffusion tomography. IEEE Transactions on Image Processing, 2001, 10, 909-922.	9.8	71
43	Sparse and Low-Rank Decomposition of a Hankel Structured Matrix for Impulse Noise Removal. IEEE Transactions on Image Processing, 2018, 27, 1448-1461.	9.8	71
44	Multi-task vision transformer using low-level chest X-ray feature corpus for COVID-19 diagnosis and severity quantification. Medical Image Analysis, 2022, 75, 102299.	11.6	69
45	Score-based diffusion models for accelerated MRI. Medical Image Analysis, 2022, 80, 102479.	11.6	68
46	Understanding Graph Isomorphism Network for rs-fMRI Functional Connectivity Analysis. Frontiers in Neuroscience, 2020, 14, 630.	2.8	65
47	Referenceâ€free singleâ€pass EPI <scp>N</scp> yquist ghost correction using annihilating filterâ€based low rank <scp>H</scp> ankel matrix (ALOHA). Magnetic Resonance in Medicine, 2016, 76, 1775-1789.	3.0	61
48	Tracing the evolution of multi-scale functional networks in a mouse model of depression using persistent brain network homology. NeuroImage, 2014, 101, 351-363.	4.2	58
49	Compressive Sampling Using Annihilating Filter-Based Low-Rank Interpolation. IEEE Transactions on Information Theory, 2017, 63, 777-801.	2.4	57
50	Low-Dose Abdominal CT Using a Deep Learning-Based Denoising Algorithm: A Comparison with CT Reconstructed with Filtered Back Projection or Iterative Reconstruction Algorithm. Korean Journal of Radiology, 2020, 21, 356.	3.4	55
51	Motion Adaptive Patch-Based Low-Rank Approach for Compressed Sensing Cardiac Cine MRI. IEEE Transactions on Medical Imaging, 2014, 33, 2069-2085.	8.9	53
52	High-speed terahertz reflection three-dimensional imaging for nondestructive evaluation. Optics Express, 2012, 20, 25432.	3.4	52
53	Unpaired Deep Learning for Accelerated MRI Using Optimal Transport Driven CycleGAN. IEEE Transactions on Computational Imaging, 2020, 6, 1285-1296.	4.4	52
54	Quantification of CMRO ₂ without hypercapnia using simultaneous near-infrared spectroscopy and fMRI measurements. Physics in Medicine and Biology, 2010, 55, 3249-3269.	3.0	48

#	Article	IF	CITATIONS
55	Artificial Intelligence in Health Care: Current Applications and Issues. Journal of Korean Medical Science, 2020, 35, e379.	2.5	46
56	AdaIN-Based Tunable CycleGAN for Efficient Unsupervised Low-Dose CT Denoising. IEEE Transactions on Computational Imaging, 2021, 7, 73-85.	4.4	44
57	A Self-Referencing Level-Set Method for Image Reconstruction from Sparse Fourier Samples. International Journal of Computer Vision, 2002, 50, 253-270.	15.6	42
58	Sparse SPM: Group Sparse-dictionary learning in SPM framework for resting-state functional connectivity MRI analysis. NeuroImage, 2016, 125, 1032-1045.	4.2	39
59	Compressed sensing fMRI using gradient-recalled echo and EPI sequences. NeuroImage, 2014, 92, 312-321.	4.2	38
60	Lipschitz-Killing curvature based expected Euler characteristics for p-value correction in fNIRS. Journal of Neuroscience Methods, 2012, 204, 61-67.	2.5	37
61	Optimal Transport Driven CycleGAN for Unsupervised Learning in Inverse Problems. SIAM Journal on Imaging Sciences, 2020, 13, 2281-2306.	2.2	37
62	Structured Low-Rank Algorithms: Theory, Magnetic Resonance Applications, and Links to Machine Learning. IEEE Signal Processing Magazine, 2020, 37, 54-68.	5.6	37
63	Unsupervised Deformable Image Registration Using Cycle-Consistent CNN. Lecture Notes in Computer Science, 2019, , 166-174.	1.3	37
64	MRI artifact correction using sparse + lowâ€rank decomposition of annihilating filterâ€based hankel matrix. Magnetic Resonance in Medicine, 2017, 78, 327-340.	3.0	36
65	Reconstruction of multicontrast MR images through deep learning. Medical Physics, 2020, 47, 983-997.	3.0	36
66	3D high-density localization microscopy using hybrid astigmatic/ biplane imaging and sparse image reconstruction. Biomedical Optics Express, 2014, 5, 3935.	2.9	35
67	High-speed terahertz reflection three-dimensional imaging using beam steering. Optics Express, 2015, 23, 5027.	3.4	34
68	CycleGAN denoising of extreme low-dose cardiac CT using wavelet-assisted noise disentanglement. Medical Image Analysis, 2021, 74, 102209.	11.6	34
69	Unsupervised CT Metal Artifact Learning Using Attention-Guided Î ² -CycleGAN. IEEE Transactions on Medical Imaging, 2021, 40, 3932-3944.	8.9	33
70	Fully 3D iterative scatter-corrected OSEM for HRRT PET using a GPU. Physics in Medicine and Biology, 2011, 56, 4991-5009.	3.0	31
71	CycleGAN With a Blur Kernel for Deconvolution Microscopy: Optimal Transport Geometry. IEEE Transactions on Computational Imaging, 2020, 6, 1127-1138.	4.4	31
72	Assessing the importance of magnetic resonance contrasts using collaborative generative adversarial networks. Nature Machine Intelligence, 2020, 2, 34-42.	16.0	31

#	Article	IF	CITATIONS
73	Topological persistence vineyard for dynamic functional brain connectivity during resting and gaming stages. Journal of Neuroscience Methods, 2016, 267, 1-13.	2.5	30
74	Deep learning STEM-EDX tomography of nanocrystals. Nature Machine Intelligence, 2021, 3, 267-274.	16.0	30
75	Unsupervised Deep Learning Methods for Biological Image Reconstruction and Enhancement: An overview from a signal processing perspective. IEEE Signal Processing Magazine, 2022, 39, 28-44.	5.6	30
76	Unsupervised Denoising for Satellite Imagery Using Wavelet Directional CycleGAN. IEEE Transactions on Geoscience and Remote Sensing, 2021, 59, 6823-6839.	6.3	29
77	Asymptotic global confidence regions in parametric shape estimation problems. IEEE Transactions on Information Theory, 2000, 46, 1881-1895.	2.4	28
78	AIM 2020 Challenge on Learned Image Signal Processing Pipeline. Lecture Notes in Computer Science, 2020, , 152-170.	1.3	26
79	Cramer-Rao bounds for parametric shape estimation in inverse problems. IEEE Transactions on Image Processing, 2003, 12, 71-84.	9.8	25
80	Improving Noise Robustness in Subspace-Based Joint Sparse Recovery. IEEE Transactions on Signal Processing, 2012, 60, 5799-5809.	5.3	25
81	Beyond Born-Rytov limit for super-resolution optical diffraction tomography. Optics Express, 2017, 25, 30445.	3.4	25
82	Unpaired MR Motion Artifact Deep Learning Using Outlier-Rejecting Bootstrap Aggregation. IEEE Transactions on Medical Imaging, 2021, 40, 3125-3139.	8.9	25
83	Deep learning enables reference-free isotropic super-resolution for volumetric fluorescence microscopy. Nature Communications, 2022, 13, .	12.8	23
84	Joint sparsity-driven non-iterative simultaneous reconstruction of absorption and scattering in diffuse optical tomography. Optics Express, 2013, 21, 26589.	3.4	21
85	One network to solve all ROIs: Deep learning CT for any ROI using differentiated backprojection. Medical Physics, 2019, 46, e855-e872.	3.0	20
86	Development of digital breast tomosynthesis and diffuse optical tomography fusion imaging for breast cancer detection. Scientific Reports, 2020, 10, 13127.	3.3	20
87	Variational Formulation of Unsupervised Deep Learning for Ultrasound Image Artifact Removal. IEEE Transactions on Ultrasonics, Ferroelectrics, and Frequency Control, 2021, 68, 2086-2100.	3.0	20
88	Compressed Sensing Shape Estimation of Star-Shaped Objects in Fourier Imaging. IEEE Signal Processing Letters, 2007, 14, 750-753.	3.6	19
89	Sparsity driven metal part reconstruction for artifact removal in dental CT. Journal of X-Ray Science and Technology, 2011, 19, 457-475.	1.0	19
90	Metal artifact reduction in CT by identifying missing data hidden in metals. Journal of X-Ray Science and Technology, 2013, 21, 357-372.	1.0	19

#	Article	IF	CITATIONS
91	Fully iterative scatter corrected digital breast tomosynthesis using GPUâ€based fast Monte Carlo simulation and composition ratio update. Medical Physics, 2015, 42, 5342-5355.	3.0	19
92	Asymptotic Global Confidence Regions for 3-D Parametric Shape Estimation in Inverse Problems. IEEE Transactions on Image Processing, 2006, 15, 2904-2919.	9.8	18
93	kâ€Space deep learning for referenceâ€free EPI ghost correction. Magnetic Resonance in Medicine, 2019, 82, 2299-2313.	3.0	18
94	Self-evolving vision transformer for chest X-ray diagnosis through knowledge distillation. Nature Communications, 2022, 13, .	12.8	18
95	Cycle-Free CycleGAN Using Invertible Generator for Unsupervised Low-Dose CT Denoising. IEEE Transactions on Computational Imaging, 2021, 7, 1354-1368.	4.4	17
96	Interior Tomography Using 1D Generalized Total Variation. Part I: Mathematical Foundation. SIAM Journal on Imaging Sciences, 2015, 8, 226-247.	2.2	16
97	Continuous Conversion of CT Kernel Using Switchable CycleGAN With AdaIN. IEEE Transactions on Medical Imaging, 2021, 40, 3015-3029.	8.9	16
98	DeepRegularizer: Rapid Resolution Enhancement of Tomographic Imaging Using Deep Learning. IEEE Transactions on Medical Imaging, 2021, 40, 1508-1518.	8.9	16
99	Deep learning model for diagnosing gastric mucosal lesions using endoscopic images: development, validation, and method comparison. Gastrointestinal Endoscopy, 2022, 95, 258-268.e10.	1.0	16
100	Improving the Reliability of Pharmacokinetic Parameters at Dynamic Contrast-enhanced MRI in Astrocytomas: A Deep Learning Approach. Radiology, 2020, 297, 178-188.	7.3	15
101	Interior Tomography Using 1D Generalized Total Variation. Part II: Multiscale Implementation. SIAM Journal on Imaging Sciences, 2015, 8, 2452-2486.	2.2	14
102	Wholeâ€brain perfusion imaging with balanced steadyâ€state free precession arterial spin labeling. NMR in Biomedicine, 2016, 29, 264-274.	2.8	14
103	Accuracy improvement of quantification information using super-resolution with convolutional neural network for microscopy images. Biomedical Signal Processing and Control, 2020, 58, 101846.	5.7	14
104	Computational MRI: Compressive Sensing and Beyond [From the Guest Editors]. IEEE Signal Processing Magazine, 2020, 37, 21-23.	5.6	14
105	Missing Cone Artifact Removal in ODT Using Unsupervised Deep Learning in the Projection Domain. IEEE Transactions on Computational Imaging, 2021, 7, 747-758.	4.4	14
106	Optical Coherence Tomography of Plaque Erosion. Journal of the American College of Cardiology, 2021, 78, 1266-1274.	2.8	14
107	Coherent optical computing for T-ray imaging. Optics Letters, 2010, 35, 508.	3.3	12
108	Improving M-SBL for Joint Sparse Recovery Using a Subspace Penalty. IEEE Transactions on Signal Processing, 2015, 63, 6595-6605.	5.3	12

#	Article	IF	CITATIONS
109	Deep Learning for Accelerated Ultrasound Imaging. , 2018, , .		12
110	Deep Learning-Based Universal Beamformer for Ultrasound Imaging. Lecture Notes in Computer Science, 2019, , 619-627.	1.3	12
111	A novel k-space annihilating filter method for unification between compressed sensing and parallel MRI. , 2015, , .		11
112	Single channel blind image deconvolution from radially symmetric blur kernels. Optics Express, 2007, 15, 3791.	3.4	10
113	Group sparse dictionary learning and inference for resting-state fMRI analysis of Alzheimer'S disease. , 2013, , .		10
114	Two-Dimensional Elastic Scattering Coefficients and Enhancement of Nearly Elastic Cloaking. Journal of Elasticity, 2017, 128, 203-243.	1.9	10
115	Geometric Approaches to Increase the Expressivity of Deep Neural Networks for MR Reconstruction. IEEE Journal on Selected Topics in Signal Processing, 2020, 14, 1292-1305.	10.8	10
116	Unpaired Training of Deep Learning tMRA for Flexible Spatio-Temporal Resolution. IEEE Transactions on Medical Imaging, 2021, 40, 166-179.	8.9	10
117	Two-stage deep learning for accelerated 3D time-of-flight MRA without matched training data. Medical Image Analysis, 2021, 71, 102047.	11.6	10
118	PyNET-CA: Enhanced PyNET with Channel Attention for End-to-End Mobile Image Signal Processing. Lecture Notes in Computer Science, 2020, , 202-212.	1.3	10
119	Performance evaluation of accelerated functional MRI acquisition using compressed sensing. , 2009, , .		9
120	Compressed sensing pulse-echo mode terahertz reflectance tomography. Optics Letters, 2009, 34, 3863.	3.3	9
121	Dynamic sparse support tracking with multiple measurement vectors using compressive MUSIC. , 2012, , \cdot		9
122	Compressive dynamic aperture B-mode ultrasound imaging using annihilating filter-based low-rank interpolation. , 2016, , .		9
123	A Mathematical Framework for Deep Learning in Elastic Source Imaging. SIAM Journal on Applied Mathematics, 2018, 78, 2791-2818.	1.8	9
124	BMC Biomedical Engineering: a home for all biomedical engineering research. BMC Biomedical Engineering, 2019, 1, 1.	2.6	8
125	Optimal Transport Structure of CycleGAN for Unsupervised Learning for Inverse Problems. , 2020, , .		8
126	Blind Deconvolution Microscopy Using Cycle Consistent CNN with Explicit PSF Layer. Lecture Notes in Computer Science, 2019, , 173-180.	1.3	8

#	Article	IF	CITATIONS
127	Sampling scheme optimization for diffuse optical tomography based on data and image space rankings. Journal of Biomedical Optics, 2016, 21, 106004.	2.6	7
128	Sparse-view X-ray spectral CT reconstruction using annihilating filter-based low rank hankel matrix approach. , 2016, , .		7
129	A Joint Sparse Recovery Framework for Accurate Reconstruction of Inclusions in Elastic Media. SIAM Journal on Imaging Sciences, 2017, 10, 1104-1138.	2.2	7
130	Topological sensitivity based far-field detection of elastic inclusions. Results in Physics, 2018, 8, 442-460.	4.1	7
131	Universal Plane-Wave Compounding for High Quality US Imaging Using Deep Learning. , 2019, , .		7
132	Differentiated Backprojection Domain Deep Learning for Conebeam Artifact Removal. IEEE Transactions on Medical Imaging, 2020, 39, 3571-3582.	8.9	7
133	Deep learning–based denoising algorithm in comparison to iterative reconstruction and filtered back projection: a 12-reader phantom study. European Radiology, 2021, 31, 8755-8764.	4.5	7
134	Compressive MUSIC with optimized partial support for joint sparse recovery. , 2011, , .		6
135	Switchable and Tunable Deep Beamformer Using Adaptive Instance Normalization for Medical Ultrasound. IEEE Transactions on Medical Imaging, 2022, 41, 266-278.	8.9	6
136	Terahertz substance imaging by waveform shaping. Optics Express, 2012, 20, 20783.	3.4	5
137	A unified statistical framework for material decomposition using multienergy photon counting xâ€ray detectors. Medical Physics, 2013, 40, 091913.	3.0	5
138	Translational motion correction algorithm for truncated cone-beam CT using opposite projections. Journal of X-Ray Science and Technology, 2017, 25, 927-944.	1.0	5
139	Grid-Free Localization Algorithm Using Low-Rank Hankel Matrix for Super-Resolution Microscopy. IEEE Transactions on Image Processing, 2018, 27, 4771-4786.	9.8	5
140	Quantitative susceptibility map reconstruction using annihilating filterâ€based lowâ€rank Hankel matrix approach. Magnetic Resonance in Medicine, 2020, 83, 858-871.	3.0	5
141	Unsupervised Deconvolution Neural Network for High Quality Ultrasound Imaging. , 2020, , .		5
142	DeepPhaseCut: Deep Relaxation in Phase for Unsupervised Fourier Phase Retrieval. IEEE Transactions on Pattern Analysis and Machine Intelligence, 2022, 44, 9931-9943.	13.9	5
143	Deep Learning in Biological Image and Signal Processing [From the Guest Editors]. IEEE Signal Processing Magazine, 2022, 39, 24-26.	5.6	5
144	Unsupervised resolution-agnostic quantitative susceptibility mapping using adaptive instance normalization. Medical Image Analysis, 2022, 79, 102477.	11.6	5

JONG CHUL YE

#	Article	IF	CITATIONS
145	Low-Dose Sparse-View HAADF-STEM-EDX Tomography of Nanocrystals Using Unsupervised Deep Learning. ACS Nano, 2022, 16, 10314-10326.	14.6	5
146	Compressed sensing metal artifact removal in dental CT. , 2009, , .		4
147	Compressed Sensing for fMRI: Feasibility Study on the Acceleration of Non-EPI fMRI at 9.4T. BioMed Research International, 2015, 2015, 1-24.	1.9	4
148	Fast live cell imaging at nanometer scale using annihilating filter-based low-rank Hankel matrix approach. Proceedings of SPIE, 2015, , .	0.8	4
149	A Unified Sparse Recovery and Inference Framework for Functional Diffuse Optical Tomography Using Random Effect Model. IEEE Transactions on Medical Imaging, 2015, 34, 1602-1615.	8.9	4
150	Patch based low rank structured matrix completion for accelerated scanning microscopy. , 2015, , .		4
151	Reusability report: Feature disentanglement in generating a three-dimensional structure from a two-dimensional slice with sliceGAN. Nature Machine Intelligence, 2021, 3, 861-863.	16.0	4
152	Exact reconstruction formula for diffuse optical tomography using simultaneous sparse representation. , 2008, , .		3
153	A sparse Bayesian learning for highly accelerated dynamic MRI. , 2010, , .		3
154	Sparse and low-rank decomposition of MR artifact images using annihilating filter-based Hankel matrix. , 2016, , .		3
155	Framelet denoising for low-dose CT using deep learning. , 2018, , .		3
156	Switchable Deep Beamformer For Ultrasound Imaging Using Adain. , 2021, , .		3
157	Statistical parametric mapping of FMRI data using sparse dictionary learning. , 2010, , .		2
158	Diffuse optical tomography using generalized music algorithm. , 2011, , .		2
159	Source localization approach for functional DOT using MUSIC and FDR control. Optics Express, 2012, 20, 6267.	3.4	2
160	Corrections to "Compressive MUSIC: Revisiting the Link Between Compressive Sensing and Array Signal Processing―[Jan 12 278-301]. IEEE Transactions on Information Theory, 2013, 59, 6148-6149.	2.4	2
161	Unified Theory for Recovery of Sparse Signals in a General Transform Domain. IEEE Transactions on Information Theory, 2018, 64, 5457-5477.	2.4	2
162	Unsupervised Deep Learning For Accelerated High Quality Echocardiography. , 2021, , .		2

JONG CHUL YE

#	Article	IF	CITATIONS
163	Reference-free EPI Nyquist ghost correction using annihilating filter-based low rank hankel matrix for K-space interpolation. , 2016, , .		2
164	Convolutional Neural Networks. Mathematics in Industry, 2022, , 113-134.	0.3	2
165	Multi-Domain Unpaired Ultrasound Image Artifact Removal Using a Single Convolutional Neural Network. , 2022, , .		2
166	High resolution dynamic MRI using motion estimated and compensated compressed sensing. , 2008, , .		1
167	Sparse topological data recovery in medical images. , 2011, , .		1
168	A statistical framework for material decomposition using multi-energy photon counting x-ray detector. , 2012, , .		1
169	Low-dose limited view 4D CT reconstruction using patch-based low-rank regularization. , 2013, , .		1
170	T2 prime mapping from highly undersampled data using compressed sensing with patch based low rank penalty. , 2014, , .		1
171	Multiband dynamic compressed sensing. , 2015, , .		1
172	Improved temporal resolution of twist imaging using annihilating filter-based low rank Hankel matrix approach. , 2016, , .		1
173	Editorial: Introduction to the Issue on Domain Enriched Learning for Medical Imaging. IEEE Journal on Selected Topics in Signal Processing, 2020, 14, 1068-1071.	10.8	1
174	Contrast and Resolution Improvement of POCUS Using Self-consistent CycleGAN. Lecture Notes in Computer Science, 2021, , 158-167.	1.3	1
175	Unsupervised Learning for Acoustic Shadowing Artifact Removal in Ultrasound Imaging. , 2021, , .		1
176	Radiation Dose Reduction in Digital Mammography by Deep-Learning Algorithm Image Reconstruction: A Preliminary Study. Journal of the Korean Society of Radiology, 2022, 83, 344.	0.2	1
177	Geometry of Deep Neural Networks. Mathematics in Industry, 2022, , 195-226.	0.3	1
178	General linear model and inference for near infrared spectroscopy using global confidence region analysis. , 2008, , .		0
179	Ab initio maximum likelihood reconstruction of helical macromolecules using electron microscopy. , 2009, , .		0
180	Single channel 2-D and 3-D blind image deconvolution for circularly symmetric fir blurs. , 2009, , .		0

11

0

#	ARTICLE	IF	CITATIONS
181	Fast implementation of fully iterative scatter corrected OSEM for HRRT using GPU. , 2010, , .		0
182	A data-driven spatially adaptive sparse generalized linear model for functional MRI analysis. , 2011, , .		0
183	Iterative scatter correction for digital tomosynthesis using composition ratio update and GPU based Monte Carlo simulation. , 2012, , .		0
184	Subwavelength silicon honeycomb structure for tailored index in terahertz broadband region. , 2012, , ,		0
185	Resting-state fMRI analysis of Alzheimer's disease progress using sparse dictionary learning. , 2012, , .		0
186	Compressed sensing reconstruction of statistical parameter map for functional diffuse optical tomography. , 2012, , .		0
187	Compressive subspace fitting for multiple measurement vectors. , 2012, , .		0
188	Motion compensated compressed sensing dynamic MRI with low-rank patch-based residual reconstruction. , 2013, , .		0
189	Neuroelectromagnetic imaging of correlated sources using a novel subspace penalized sparse learning. , 2013, , .		0
190	Neuroelectromagnetic imaging of correlated sources using a novel subspace penalized sparse learning. , 2013, , .		0
191	Improving resolution of fluorescent microscopy using speckle illumination and joint sparse recovery. , 2013, , .		0
192	Subspace penalized sparse learning for joint sparse recovery. , 2013, , .		0
193	Accurate inversion of absorption and scattering in diffuse optical tomography without iterative Green's function update. , 2014, , .		0
194	Improved volumetric imaging for DCE-MRI using parallel imaging and dynamic compressed sensing. , 2014, , .		0
195	ECG-gated cardiac CT reconstruction using patch based low rank regularization. , 2014, , .		0
196	Recent progresses of accelerated MRI using annihilating filter-based low-rank interpolation. , 2016, , .		0
197	Improved Time-Resolved MRA Using k-Space Deep Learning. Lecture Notes in Computer Science, 2018, , 47-54.	1.3	0

198 Mathematical Foundations of AIM. , 2021, , 1-18.

#	Article	IF	CITATIONS
199	High Resolution Time Resolved Contrast Enhanced MR Angiography Using k-t FOCUSS. Journal of the Korean Society of Magnetic Resonance in Medicine, 2010, 14, 10.	0.1	0
200	Mathematical Foundations of AIM. , 2022, , 37-54.		0
201	Abstract 10310: Deep Learning for a Diagnosis of Plaque Erosion in Patients with Acute Coronary Syndromes. Circulation, 2021, 144, .	1.6	0